Universal properties of the Kardar-Parisi-Zhang equation with quenched columnar disorders

Astik Haldar*
Theory Division, Saha Institute of Nuclear Physics, HBNI, Calcutta 700064, India

(Received 26 December 2020; revised 1 March 2021; accepted 23 July 2021; published 9 August 2021)

Inspired by the recent results on totally asymmetric simple exclusion processes on a periodic lattice with short-ranged quenched hopping rates [A. Haldar and A. Basu, Phys. Rev. Research **2**, 043073 (2020)], we study the universal scaling properties of the Kardar-Parisi-Zhang (KPZ) equation with short-ranged quenched columnar disorder in general d dimensions. We show that there are generic propagating modes in the system that have their origin in the quenched disorder and make the system anisotropic. We argue that the presence of the propagating modes actually make the effects of the quenched disorder irrelevant, making the universal long wavelength scaling property belong to the well-known KPZ universality class. On the other hand, when these waves vanish in a special limit of the model, new universality class emerges with dimension $d = 4$ as the lower critical dimension, above which the system is speculated to admit a disorder-induced roughening transition to a perturbatively inaccessible rough phase.

DOI: 10.1103/PhysRevE.104.024109

I. INTRODUCTION

Quenched disorders are known to significantly affect the universal scaling properties of condensed matter systems and statistical models in equilibrium. For example, the universal critical properties of classical N-component spin models near their second-order phase transitions can be affected by the quenched disorder, leading to a new universality class [1,2]. On the other hand, quenched random fields can destroy the ordered phase altogether [3]. Scaling properties of interface growth models are also found to be affected by quenched disorders [4–7]. Understanding of how quenched disorders affect universal properties in nonequilibrium systems is far less understood than their equilibrium counterparts, and remains a challenging problem. Lack of any general framework to study the statistical properties of nonequilibrium systems has often prompted physicists to construct and study simple conceptual models that are easily analytically tractable, such that questions of basic principles can be answered within well-controlled approximations.

The Kardar-Parisi-Zhang equation, originally proposed as a nonlinear hydrodynamic model for surface growth phenomena [8], serves as a paradigmatic model for nonequilibrium phase transition above dimension $d > 2$. Recently, the universal scaling properties of the density fluctuations in a totally asymmetric simple exclusion process (TASEP) in a ring geometry with quenched disordered hopping rates has been studied by mapping the problem into a one-dimensional (1D) Kardar-Parisi-Zhang equation with quenched columnar disorder (disorder distributions, which depend only on position and are fixed in time) [9]. It has been shown that away from the half-filling, the quenched disorder is irrelevant, and the universal long wavelength properties of the system is identical to that of the 1D KPZ equation without any disorder. On the other hand, close to half-filling, quenched disorder is relevant, a new universality class different from the 1D KPZ universality emerges, leading to the scaling exponents taking values different from their 1D KPZ counterpart. These results qualitatively agree with the simulations performed [10–12] for driven lattice gases in presence of quenched disorder. Furthermore, it was speculated in Ref. [9], based on a simple scaling analysis and the linear instability of the Gaussian fixed point that near the analog of half-filling, the lower critical dimension might be higher than 2. This speculation makes it imperative to ask what precisely the critical dimension is, and whether it is truly the lower critical dimension (as opposed to the upper critical dimension).

In this article, we systematically generalize the 1D KPZ equation with short-ranged quenched columnar disorder [9] to d dimensions. We systematically study this equation to uncover its universal scaling properties in the long wavelength limit. Our principal results in this article are as follows. (i) The generalized d-dimensional equation does not remain invariant under Galilean transformation in presence of the disorder, and there are generic underdamped propagating waves in the system. The latter makes the system necessarily anisotropic. (ii) Surprisingly, the presence of the waves makes the disorder *irrelevant* (in a renormalization group or RG sense). As a result and very intriguingly, the Galilean invariance and isotropy are restored in the long wavelength limit; the universal scaling property naturally belongs to the d-dimensional KPZ universality class. (iii) For specific choices of the model parameters, the waves vanish and the system is isotropic. In this case the disorder is relevant (in a RG sense), and the Galilean invariance remains broken in the long wavelength limit. Consequently, the universal scaling exponents belong to a new universality class different from the pure KPZ equation. In particular, the scaling exponents at $d = 2$, relevant for surface growth phenomena, are calculated at the one-loop

*astik.haldar@gmail.com

order. We establish that $d = 4$ is the *lower critical dimension* of the model in this case, such that above $d = 4$, the model can undergo a roughening transition to a (perturbatively inaccessible) rough phase. This disorder-mediated roughening transition generalizes the well-known roughening transition of the pure KPZ equation for $d > 2$. We thus find that independent of whether waves are present or absent, the statistics of the long wavelength fluctuations are *always isotropic*. Paradoxically, the waves—when they are present and make the system anisotropic at small scales—are responsible for the emergent isotropy in the long wavelength limit. This is a prominent outcome from our study. We use a one-loop dynamic RG calculational framework for our work.

Although the KPZ equation was originally proposed as a hydrodynamic model for surface growth, it has been extensively studied as a paradigmatic model for nonequilibrium phase transition. It has also been recognized as a hydrodynamic model for other phenomena, e.g., nonequilibrium dynamics of the phase in a collection of nearly phase ordered model [13]. All these have led to extensive theoretical studies of the KPZ equation at various dimensions [14]. Likewise, the quenched disordered d-dimensional KPZ equation that we construct and study here is not only significant as a hydrodynamic model for growing surfaces in the presence of quenched disorder (with 2D as the physically relevant dimension), but is also a paradigmatic nonequilibrium quenched disordered hydrodynamic model that displays a disorder-induced roughening transition, with its implications transcending the narrow boundaries of surface growth phenomena. For a comprehensive and thorough understanding of the universal aspects of this model, it is essential to study this model theoretically in general d dimensions.

The rest of this article is organized in the following manner. We set up the hydrodynamic equations for height of growing surfaces with quenched columnar disorder in Sec. II. The KPZ universality has been discussed in Sec. III. We discuss the scaling behavior in linear theory in Sec. IV A, and then calculate the nonlinear effects on the scaling exponents by using RG framework for this quenched disordered model in rest of Sec. IV. We summarize our results in Sec. V. Some technical details are provided in the Appendix for the interested readers.

II. KPZ EQUATION WITH COLUMNAR QUENCHED DISORDER

We begin by recalling the 1D hydrodynamic equation, derived in Ref. [9] for density fluctuations in a periodic TASEP with quenched disordered hopping rates in the thermodynamic limit. The equation of motion (EoM) for density fluctuation $\phi(x,t)$ reads [9]

$$\begin{aligned}\frac{\partial\phi(x,t)}{\partial t} &= \nu\frac{\partial^2\phi(x,t)}{\partial x^2} + \lambda_1\frac{\partial\phi(x,t)}{\partial x} + \lambda_m\frac{\partial\delta m(x)}{\partial x} \\ &\quad - \frac{\lambda}{2}\frac{\partial\phi^2(x,t)}{\partial x} + \lambda_2\frac{\partial}{\partial x}[\delta m(x)\phi(x,t)] \\ &\quad - \lambda_3\frac{\partial}{\partial x}[\delta m(x)\phi^2(x,t)] + \frac{\partial f(x,t)}{\partial x}. \end{aligned} \tag{1}$$

Here, ν is a diffusion coefficient, λ, λ_m, λ_1, λ_2, λ_3 are different model parameters. In particular, λ_1, λ_2 are both proportional to $(2\rho_0 - 1)$ where ρ_0 is the mean particle density. Hence, λ_1, λ_2 vanish in the half-filled limit ($\rho_0 = 1/2$) whereas those have nonzero value for away from the half-filled limit [9]. Furthermore, $m(x)$ is the random quenched disorder that has its origin in the quenched disorder hopping rates in the underlying lattice-gas TASEP model. To make precise connections with TASEP on a ring geometry, periodic boundary conditions on the fields and the noises together with $x \in [0, L]$, along with the thermodynamic limit $L \to \infty$ are to be assumed. As explained in Ref. [9], density fluctuation $\phi(x,t)$ is driven by two conserved stochastic variables: quenched noise $\partial_x\delta m(x)$ and annealed noise $\partial_x f(x,t)$. We write $m(x) = m_0 + \delta m(x)$, where $m_0 = \overline{m(x)}$ is the mean value of $m(x)$, and $\delta m(x)$ is local fluctuation of $m(x)$ about m_0. We assume $\delta m(x) < m_0$ to ensure $m(x)$ remains positive everywhere;[1] we choose $\delta m(x)$ to be short-ranged Gaussian distributed with a variance

$$\overline{\delta m(x)\delta m(0)} = 2\tilde{D}\delta(x); \tag{2}$$

$\tilde{D}$ is the strength of the quenched noise, and is definite positive.

Stochastic function $f(x,t)$ is an annealed noise, which is assumed to be zero mean and Gaussian distributed with a variance

$$\langle f(x,t)f(0,0)\rangle = 2D\delta(x)\delta(t). \tag{3}$$

Here, $D > 0$ is the noise strength, the analog of temperature in nonequilibrium systems. Here $\langle\ldots\rangle$ implies the averages over time-dependent noise distribution and an overline implies the averages over quenched disorder distribution. The annealed noise $f(x,t)$ models the inherent stochastic nature of the dynamics (or the update rules) of the underlying lattice-gas model, and is essentially a nonequilibrium generalization of thermal noises present in equilibrium systems at finite temperatures.

The variances of $f(x,t)$ and $\delta m(x)$ in the Fourier space are

$$\langle f(k_1,\omega_1)f(k_2,\omega_2)\rangle = 2D\delta(k_1+k_2)\delta(\omega_1+\omega_2), \tag{4a}$$

$$\overline{\delta m(k_1,\omega_1)\delta m(k_2,\omega_2)} = 2\tilde{D}\delta(k_1+k_2)\delta(\omega_1+\omega_2)\delta(\omega_1). \tag{4b}$$

Let us introduce a height variable via the transformation $\phi(x,t) = \partial_x h$. This transforms (1) to

$$\begin{aligned}\frac{\partial h(x,t)}{\partial t} &= \nu\partial_{xx}h(x,t) + \partial_x h(x,t)[\lambda_1 + \lambda_2\delta m(x)] \\ &\quad - \frac{\lambda}{2}[\partial_x h(x,t)]^2 + \lambda_2[\delta m(x)\partial_x h(x,t)] \\ &\quad - \lambda_3[\delta m(x)(\partial_x h(x,t))^2] \\ &\quad + \lambda_m\delta m(x) + f(x,t). \end{aligned} \tag{5}$$

Here $h(x,t)$, a single-valued function, is the height of the 1D surface with respect to an arbitrary baseline. Equation (5)

[1] In the lattice-gas TASEP language this condition means the local hopping rate remains positive everywhere; a negative $m(x)$ at some x means a negative hopping rate at that point, a possibility excluded in the definition of the lattice-gas model. However, a negative $m(x)$ is acceptable in an equivalent surface growth model.

gives the dynamics of a growing 1D surface with quenched columnar disorder. Some general comments on the structure of (5) are in order: The first term on the first line of the right-hand side (rhs) of Eq. (5) is the standard diffusive term, identical to its counterpart in the pure KPZ equation. The second term on the first line of the rhs is a first-order spatial derivative term of h with a coefficient that depends on the quenched disorder. In the absence of the quenched disorder, this coefficient is a constant and can be removed by a Galilean transformation [14,15], and hence does not appear in the pure KPZ equation. The second and third lines of the rhs contain three nonlinear terms; the first one is the well-known nonlinear term of the pure KPZ equation and another two depend on the quenched disorder. The two terms on the fourth line of the rhs act as the external sources, one of which, i.e., $\lambda_m \delta m(x)$, is time-independent, i.e., quenched and has no analog in the pure KPZ equation; the second one $f(x,t)$ is time-dependent and hence annealed, models the inherent stochastic nature of the microscopic dynamics, and survives in the pure KPZ limit. We further note that, when $\lambda_1 = 0 = \lambda_2$, Eq. (5) is invariant under inversion of space, i.e., under $x \to -x$, whereas for $\lambda_1 \neq 0$, $\lambda_2 \neq 0$, it is not, due to the presence of the propagating waves. These correspond, respectively, to near the half-filled and away from the half-filled limits for density fluctuation in Eq. (1).

We now generalize the problem to a d-dimensional growing surface in presence of columnar quenched disorder. This can be done in several ways. We generalize in a way to ensure that the d-dimensional generalized equation has a definite symmetry, and reduces to the 1D case in a simple and unambiguous way. Noticing that there are two terms (with coefficients λ_1, λ_2) containing single spatial derivative on h in (5), which imply the absence of the space inversion symmetry in EoM, we generalize the EoM of $h(\mathbf{x},t)$ to d dimensions by assuming breakdown of the inversion symmetry along one particular dimension, while the system remains inversion symmetric along all other $(d-1)$ directions. We use $\parallel$ as subscript to denote the special direction in which the inversion symmetry is absent. The generalized EoM for $h(\mathbf{x},t)$ ($\mathbf{x}$ now refers as position on d-dimensional surface) has the generic form

$$\frac{\partial h}{\partial t} = \nu \nabla^2 h + \lambda_1 \partial_\parallel h + \lambda_m \delta m - \frac{\lambda}{2}[\nabla h]^2 + \lambda_2 [\delta m \partial_\parallel h] - \lambda_3 [\delta m (\nabla h)^2] + f. \tag{6}$$

It is clear that Eq. (6) has a lower symmetry than the d-dimensional KPZ equation. It is rotationally invariant in the $(d-1)$-dimensional subspace, which excludes the $\parallel$ direction, unlike the d-dimensional KPZ equation that is rotationally invariant in the full d-dimensional space. It is instructive to write down the Burgers version [15,16] of Eq. (6) for a quenched disorder Burgers velocity $\mathbf{v}$ by using the transformation $\mathbf{v} = \nabla h$:

$$\frac{\partial \mathbf{v}}{\partial t} = \nu \nabla^2 \mathbf{v} + \lambda_1 \nabla v_\parallel + \lambda_m \nabla \delta m - \frac{\lambda}{2} \nabla [v]^2 + \lambda_2 \nabla [\delta m v_\parallel] - \lambda_3 \nabla [\delta m (v)^2] + \nabla f. \tag{7}$$

The variances of the noises in d-dimensional space are just the direct generalizations, respectively, of (2) and (3):

$$\overline{\delta m(\mathbf{x}) \delta m(0)} = 2\tilde{D}\delta^d(\mathbf{x}). \tag{8a}$$

$$\langle f(\mathbf{x},t) f(0,0)\rangle = 2D\delta^d(\mathbf{x})\delta(t). \tag{8b}$$

Due to the presence of quenched disorders, Eq. (6) does not remain invariant under the Galilean transformation $\mathbf{x} \mapsto \mathbf{x} + \mathbf{v}_0 t$, $t \mapsto t$, $h(\mathbf{x}, t \mapsto h(\mathbf{x} + \mathbf{v}_0 t) + \mathbf{v}_0 \cdot \mathbf{x})$. In Eq. (6) the term with linear derivative $\lambda_1 \partial_\parallel h$ implies the existence of underdamped propagating modes. The surface would be anisotropic due to presence of the propagating modes with picking up a specific direction, that without any loss of generality is assumed to be along the x direction, i.e., the parallel direction $x_\parallel$ is identified with the x direction. In the absence of any quenched disorder [$\delta m(\mathbf{x}) = 0$], Eq. (10) reduces to the well-known KPZ equation.

Notice that the height fluctuation governed by Eq. (6) is driven by quenched [$\delta m(\mathbf{x})$] and annealed [$f(\mathbf{x},t)$] noises, which scale in differently under rescaling of space and time (see below). Decomposing $h(\mathbf{x},t) = h_1(\mathbf{x}) + h_2(\mathbf{x},t)$, a time-independent $h_1(\mathbf{x})$ and a time-dependent $h_2(\mathbf{x},t)$ is a convenient choice that allows us to extract the fluctuation corrections systematically. Furthermore, this choice allows us to enlarge the effective parameter space [see the text below Eq. (10)], which in the RG procedure eventually produce fixed points and which can be interpreted straightforwardly [9]. Time-independent function $h_1(\mathbf{x})$ then satisfies

$$-\nu_\psi \nabla^2 h_1 - \lambda_{1\psi} \partial_\parallel h_1 - \lambda_m \delta m + \frac{\lambda_\psi}{2}(\nabla h_1)^2 - \lambda_{2\psi}[\delta m(\partial_\parallel h_1)] + \lambda_{3\psi}[\delta m (\nabla h_1)^2] = 0. \tag{9}$$

Time-dependent function $h_2(\mathbf{x},t)$ satisfies

$$\frac{\partial h_2}{\partial t} = \nu_\rho \nabla^2 h_2 + \lambda_{1\rho} \partial_\parallel h_2 - \frac{\lambda_\rho}{2}(\nabla h_2)^2 + \lambda_{2\rho}[\delta m(\partial_\parallel h_2)] - \lambda_{\rho\psi}(\nabla h_1)\cdot(\nabla h_2) - \lambda_{3\rho}[\delta m (\nabla h_2)^2] - \lambda_{3\rho\psi}[\delta m \nabla h_1 \cdot \nabla h_2] + f. \tag{10}$$

Here, we use different sets of model parameters associated h_1 and h_2 to allow for different scalings of h_1 and h_2 in long wavelength limit. The parameters ν_ψ, ν_ρ are directly proportional to ν; similarly λ_ψ, λ_ρ, $\lambda_{\rho\psi}$ are proportional to λ; $\lambda_{1\psi}$, $\lambda_{1\rho}$ are proportional to λ_1; also $\lambda_{2\psi}$, $\lambda_{2\rho}$ are proportional to λ_2 and $\lambda_{3\psi}$, $\lambda_{3\rho}$, $\lambda_{3\rho\psi}$ are proportional to λ_3. However, we treat each of these constants as independent parameters, since any simple relation between them in the bare or unrenormalized theory is not maintained by the RG procedure (see below).

Equations (9) and (10) obviously generalize the corresponding 1D equations in Ref. [9]. Field $h_1(\mathbf{x})$ represents the frozen height of a surface, which is entirely driven by the quenched disorder $\delta m(\mathbf{x})$, whereas h_2 represents the time-dependent height of a growing surface, driven by the time-dependent additive noise f. Clearly, the dynamics of the height field $h_2(\mathbf{x},t)$ in Eq. (10) is affected by the frozen height field $h_1(\mathbf{x})$ that satisfies Eq. (9), and hence by the quenched disorder.

We define two cases depending on the choices of parameters. *Case I*: Here, $\lambda_1 \neq 0$, $\lambda_2 \neq 0$ hence $\lambda_{1\psi}$, $\lambda_{1\rho}$, $\lambda_{2\psi}$, $\lambda_{2\rho}$ are nonzero, leading to the presence of propagating

modes. *Case II*: here, $\lambda_1 = 0$, $\lambda_2 = 0$ mean $\lambda_{1\psi} = \lambda_{1\rho} = \lambda_{2\psi} = \lambda_{2\rho} = 0$, propagating modes vanish and the full d-dimensional isotropic property of surface is restored. These two cases are corresponding to the away from half-filled limit and near to the half-filled limit of the periodic TASEP [9], respectively.

III. KARDAR-PARISI-ZHANG UNIVERSALITY CLASS

We first briefly review the KPZ universality before analyzing our disordered model. The KPZ equation is given by [8]

$$\frac{\partial h}{\partial t} = \nu \nabla^2 h - \frac{\lambda}{2}(\nabla h)^2 + f. \tag{11}$$

Here, $h(\mathbf{x}, t)$ is height of d-dimensional surface at any instant time t and driven by Gaussian white noise f with satisfying (8b). This model equation admits Galilean invariance due to transformation of the inertial frame. Correlation function of the height fluctuations follows the scaling in the long wavelength limit:

$$\langle [h(\mathbf{x}, t) - h(0, 0)]^2 \rangle = |\mathbf{x}|^{2\chi} \Theta(|\mathbf{x}|^z / t). \tag{12}$$

Here, χ and z are roughness and dynamic exponents for h; Θ is a dimensionless scaling function of its argument. One could find the scaling behavior of $h(\mathbf{x}, t)$ in the long time limit by defining a dimensionless coupling constant $g = \frac{\lambda^2 D}{\nu^3}$. The RG flow equation for g in the one-loop perturbative theory satisfies

$$\frac{dg}{dl} = g\left[2 - d + g\frac{4d - 6}{d}\right]. \tag{13}$$

Notice from (13) that g diverges at $d = 3/2$; furthermore, between $3/2 < d < 2$ $g = 0$, is the only physically acceptable solution. This is believed to be an artifact of the one-loop perturbation theory [17]. The Galilean invariance of the KPZ equation leads to $\chi + z = 2$, an exact relation between the scaling exponents. At one dimension, $z = 3/2$ and $\chi = 1/2$ are exactly known analytically due to the fluctuation-dissipation-theorem in the model. Coupling g grows under rescaling and is marginally relevant at $d = 2$, the lower critical dimension of the KPZ equation. The KPZ equation admits a roughening transition (smooth-to-rough phase transition) for dimensions higher than 2D; the rough phase is inaccessible in the perturbative theory. Various aspects of the KPZ equation have been studied extensively by several methods, including perturbative and nonperturbative methods. We refer the interested reader to Refs. [18–24] for details. Our studies here on the quenched columnar disordered KPZ equation complement and extend the general studies of the KPZ equation.

IV. UNIVERSAL PROPERTIES AND SCALING BEHAVIOUR

The autocorrelation functions of $h_1(\mathbf{x})$ and $h_2(\mathbf{x}, t)$ are characterized by the universal scaling exponents. The autocorrelation functions are given by

$$C_1(\mathbf{x}) \equiv \overline{[h_1(\mathbf{x}) - h_1(0)]^2} = |x_\parallel|^{2\chi_1} f_1\left(\frac{|\mathbf{x}|_\perp^{\mu_1}}{x_\parallel}\right), \tag{14}$$

$$C_2(\mathbf{x}, t) \equiv \overline{\langle [h_2(\mathbf{x}, t) - h_2(0, 0)]^2 \rangle} = |x_\parallel|^{2\chi_2} f_2\left(|x_\parallel|^z / t, \frac{|\mathbf{x}|_\perp^{\mu_2}}{x_\parallel}\right). \tag{15}$$

Here, f_1 and f_2 are two dimensionless scaling functions of their arguments; $\mathbf{x} = (x_\parallel, \mathbf{x}_\perp)$ with $x_\parallel$ being the direction of propagation of the traveling waves and $\mathbf{x}_\perp$ being $d - 1$ transverse directions to the propagating direction of waves. The scaling functions represent the generic anisotropy in the presence of the propagating waves. Scaling exponents χ_1 and χ_2 are roughness exponents for h_1 and h_2, respectively, and z is dynamic exponent of h_2; exponents μ_1, μ_2 are the anisotropy exponents with $\mu_2 = 1$ in the pure d-dimensional KPZ equation (since it is fully isotropic).

A. Linear theory

The equal-time autocorrelation functions of $h_1(\mathbf{x})$ and $h_2(\mathbf{x}, t)$ can be written down exactly in the linear theory using the linear terms in (9) and (10). These in the Fourier space for *Case I* are

$$\langle |h_1(\mathbf{k})|^2 \rangle \simeq \frac{2\tilde{D}\lambda_m^2}{\lambda_{1\psi}^2 k_\parallel^2 + \nu_\psi^2 k_\perp^4}, \tag{16a}$$

$$\langle |h_2(\mathbf{k}, t)|^2 \rangle = \frac{D}{\nu_\rho k^2}, \tag{16b}$$

where in (16a) we have ignored $k_\parallel^4$ in comparison with $k_\parallel^2$ in the long wavelength limit. Naturally, the exponents $\chi_1 = (2 - d)/2$ and $\chi_2 = (2 - d)/2$ in the linear theory are known exactly. Furthermore, we identify that $\mu_1 = 2$ and $\mu_2 = 1$ in the linear theory. See Ref. [14] for the linear analysis on the KPZ equation.

Similarly, the equal-time autocorrelation functions for *Case II* are also known exactly in the linear theory. These are given by

$$\langle |h_1(\mathbf{k})|^2 \rangle = \frac{2\tilde{D}\lambda_m^2}{\nu_\psi^2 k^4}. \tag{17a}$$

$$\langle |h_2(\mathbf{k}, t)|^2 \rangle = \frac{D}{\nu_\rho k^2} \tag{17b}$$

in the Fourier space. We thus find that $\chi_1 = (4 - d)/2$ and $\chi_2 = (2 - d)/2$ in linear theory; in this case $\mu_1 = 1 = \mu_2$. z remains at 2 and χ_2 has the same value in the linear theory in both the cases.

B. Nonlinear effects

The nonlinear terms in (9) and (10) may change the scaling exponents found in the linear theory. The exponents can no longer be found exactly in the presence of the nonlinear terms. Furthermore, naïve perturbation theory produces diverging corrections to the model parameters. To handle these divergences systematically, we here use perturbative dynamical RG approach to find the effects of anharmonic terms in scaling exponents for long wavelength limit.

The RG method is well documented in the literature [14,15,25]; we briefly outline the steps of the RG analysis. The momentum shell dynamic RG consists of few steps, at first the fields are expressed as the sum of low and high wave-vector modes: $h_1(\mathbf{q}) = h_1^<(\mathbf{q}) + h_1^>(\mathbf{q})$ and $h_2(\mathbf{q}, \omega) = h_2^<(\mathbf{q}, \omega) + h_2^>(\mathbf{q}, \omega)$. Here $<$, $>$ represent low and high wave-vector modes, respectively. Let the upper wave-vector cutoff be $\Lambda \sim 1/a$, where a is the microscopic length scale in the system.

We integrate out the high wave-vector Fourier modes of fields having wave vectors $\Lambda e^{-\delta l} < |\mathbf{q}| < \Lambda$. This integration can only be done perturbatively, which are represented diagrammatically by the Feynman diagrams, which in turn are given in the Appendices B and C. This integration reduces the upper cutoff of wave vector to $\Lambda e^{-\delta l}$ from Λ, and then we restore the upper limit of wave vector to Λ by rescaling wave vector by $\mathbf{q}' = \mathbf{q}e^{\delta l}$, along with the frequency by $\omega' = \omega e^{z\delta l}$, where z is the dynamic exponent. The long wavelength parts of the fields are also rescaled; the necessary details are available in Appendix A. This procedure ultimately yields the RG flow equations, which in turn gives the RG fixed points.

C. Universality class of Case I

In this case, the surface is anisotropic due to the existence of the traveling waves with nonzero $\lambda_{1\psi}$, $\lambda_{1\rho}$. We write the model equations keeping the most relevant terms in the long wavelength limit below.

$$-\nu_\psi \nabla^2 h_1 - \lambda_{1\psi}\partial_\parallel h_1 - \lambda_m \delta m + \frac{\lambda_\psi}{2}(\nabla h_1)^2 - \lambda_{2\psi}[\delta m(\partial_\parallel h_1)] = 0, \tag{18}$$

and

$$\frac{\partial h_2}{\partial t} = \nu_\rho \nabla^2 h_2 + \lambda_{1\rho}\partial_\parallel h_2 - \frac{\lambda_\rho}{2}(\nabla h_2)^2 + \lambda_{2\rho}[\delta m(\partial_\parallel h_2)] - \lambda_{\rho\psi}(\nabla h_1)\cdot(\nabla h_2) + f. \tag{19}$$

The perturbative corrections of these parameters, which involve disorder (proportional to $\tilde{D}$) are finite; infrared divergent corrections are due to the pure KPZ nonlinear term $[\frac{\lambda_\rho}{2}(\nabla h_2)^2]$ only, see Appendix B. Now to determine the scaling of the dimensionless effective coupling constants near the Gaussian fixed point, that depend upon the disorder variance $\tilde{D}$. These are $a_0 = \frac{\lambda_\psi^2 \tilde{D}\lambda_m^2}{\lambda_{1\psi}^4}$, $a_1 = \frac{\tilde{D}\lambda_{2\psi}^2}{\lambda_{1\psi}^2}$, $a_2 = \frac{\lambda_{\rho\psi}^2 \tilde{D}\lambda_m^2}{\lambda_{1\rho}^2\lambda_{1\psi}^2}$, $a_3 = \frac{\lambda_{2\rho}^2\tilde{D}}{\lambda_{1\rho}^2}$, $a_4 = \frac{\lambda_\psi\lambda_{2\psi}\tilde{D}\lambda_m}{\lambda_{1\psi}^3}$. Under the rescaling of the wave vector, frequency, and the fields, the flow of these near the Gaussian fixed point [9]

$$\frac{da_0}{dl} = -da_0,\ \frac{da_1}{dl} = -da_1,\ \frac{da_2}{dl} = -da_2,\ \frac{da_3}{dl} = -da_3,\ \frac{da_4}{dl} = -da_4. \tag{20}$$

Thus all these coupling constants are irrelevant near the Gaussian fixed point at all dimensions. The Galilean invariance of the dynamics of $h_2(\mathbf{x}, t)$ is restored in the long wavelength limit due to the irrelevance of the quenched disorder. The flow of the dimensionless coupling constant $\tilde{g} = \frac{\lambda_\rho^2 D}{\nu_\rho^3}$, which appears in the pure KPZ problem as well, near the Gaussian fixed point is

$$\frac{d\tilde{g}}{dl} = \tilde{g}[2-d]. \tag{21}$$

This is unstable for $d < 2$, but stable for $d > 2$. At any rate, even for $d > 2$, $\tilde{g}$ remains more relevant near the Gaussian fixed point than the other dimensionless coupling constants as defined above, all of which have their origins in the disorder. We can thus conclude that disorder is irrelevant (in a RG sense) in the long wavelength limit at all dimensions for *Case I*. This immediately implies that the long wavelength scaling is governed by the KPZ nonlinearity with the universal scaling belonging to the KPZ universality class. Thus, a roughening transition is expected at $d > 2$, just as it is for the pure KPZ equation, to a rough phase identical to that for the pure KPZ equation, whose scaling properties are not accessible to the standard perturbative calculations. Furthermore and related to what we have just concluded, isotropy is restored in the long wavelength limit of the fluctuations of h_2. This implies $\mu_2 = 1$ in the renormalized equation, as in the pure KPZ equation. This generalizes one of the conclusions of Ref. [9] valid for 1D. We therefore conclude that while the Gaussian fixed point is stable with respect to perturbations by the quenched disorder, the pure KPZ nonlinearity (with coupling $\tilde{g}$) remains relevant and determines the universal scaling properties. Thus the long wavelength properties of the model is given by the KPZ universality class. Therefore lower critical dimension is 2 and a roughening transition (i.e., a smooth-to-rough transition) exists as in the pure KPZ equation. The upper critical dimension of Case I, identical to that for the pure KPZ equation, is not known. It is speculated to be 4 by some authors [26–30], although it remains debatable till the date.

D. Universality class of Case II

We now discuss the universal scaling properties of Case II. In this case, the underdamped propagating modes vanish (since $\lambda_1\rho = 0$) in the dynamics of $h_2(\mathbf{x}, t)$ as discussed before in Sec. II. Thus the surface is isotropic. We write down below the model equations keeping most relevant nonlinear terms:

$$-\nu_\psi \nabla^2 h_1 - \lambda_m \delta m + \frac{\lambda_\psi}{2}(\nabla h_1)^2 = 0. \tag{22}$$

$$\frac{\partial h_2}{\partial t} = \nu_\rho \nabla^2 h_2 - \lambda_{\rho\psi}[\nabla h_1 \cdot \nabla h_2] + f. \tag{23}$$

The naïve perturbative fluctuation corrections to the model parameters diverge in the long wavelength limit, which can be systematically handled within the RG framework. Here we perform one loop RG analysis; fluctuation corrections of parameters are represented by the one loop Feynman diagrams whose details are available in Appendix C. The flow equations of the model parameters are

$$\frac{d\nu_\psi}{dl} = \nu_\psi\left[d - 2 + \left(\frac{2}{d} - 1\right)g_1\right]. \tag{24a}$$

$$\frac{d\lambda_m}{dl} = \lambda_m\left[-\chi_1 - \frac{3d}{2} + \frac{g_1}{2}\right]. \tag{24b}$$

$$\frac{d\lambda_\psi}{dl} = \lambda_\psi\left[-d - 2 + \chi_1 - \frac{2g_1}{d}\right]. \tag{24c}$$

$$\frac{d\nu_\rho}{dl} = \nu_\rho\left[z - 2 + \left(\frac{2}{d} - 1\right)g_2\right]. \tag{24d}$$

$$\frac{dD}{dl} = D[-d + z - 2\chi_2 + 2g_2]. \tag{24e}$$

$$\frac{d\lambda_{\rho\psi}}{dl} = \lambda_{\rho\psi}\left[z - 2 + \chi_1 - \frac{2g_2}{d}\right]. \tag{24f}$$

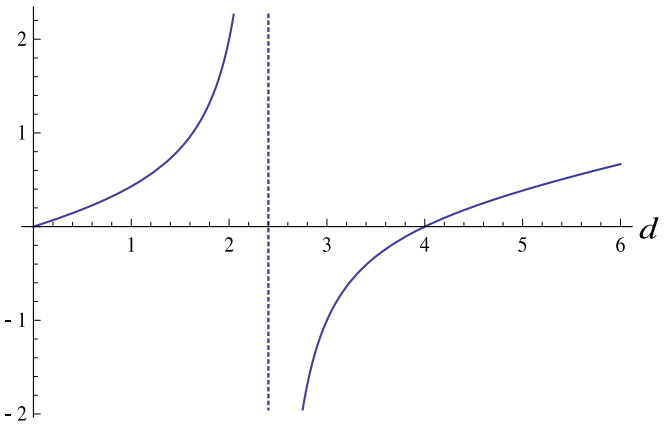

FIG. 1. Nontrivial fixed point value of g_1 as a function of d (surface dimension) in one loop calculation. This is also same for g_2; see text.

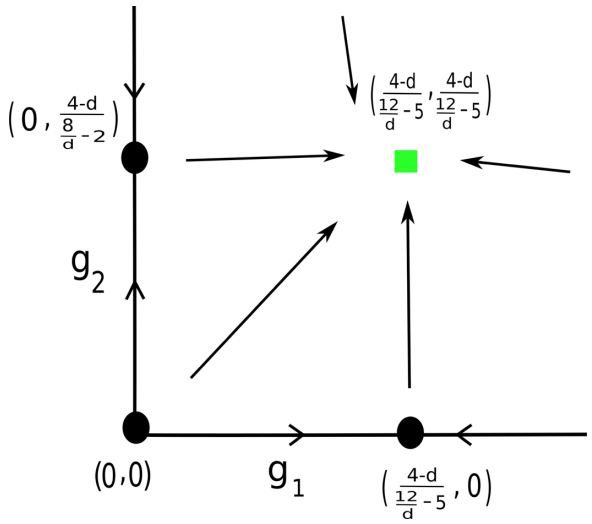

FIG. 2. Schematic RG flow diagram for $d < 4$. Stable and unstable fixed points are shown; flow lines indicate the direction of the RG flows towards stable FP (see text).

Here, the dimensionless coupling constants are $g_1 = \frac{\lambda_\psi^2 \tilde{D} \lambda_m^2}{\nu_\psi^4} \frac{\Omega_d}{(2\pi)^4}$, $g_2 = \frac{\lambda_{\rho\psi}^2 \tilde{D} \lambda_m^2}{\nu_\psi^2 \nu_\rho^2} \frac{\Omega_d}{(2\pi)^4}$ involving $\tilde{D}$, where Ω_d is angular part of the d-dimensional loop integrals. The flow equations of g_1 and g_2 are

$$\frac{dg_1}{dl} = g_1[4 - d + (5 - 12/d)g_1], \tag{25}$$

$$\frac{dg_2}{dl} = g_2[4 - d + (2 - 8/d)g_2 + (3 - 4/d)g_1]. \tag{26}$$

Flow equations (25) and (26) clearly reveal that $d = 4$ is the critical dimension of both g_1 and g_2. Let us now calculate the fixed point (FP) values of g_1 and g_2 at different dimensions by setting $dg_1/dl = 0 = dg_2/dl$. The Gaussian FP is $g_1^* = 0 = g_2^*$, furthermore one can find easily nontrivial FP as $g_1^* = \frac{4-d}{12/d-5}$ from (25) and using this in (26) $g_2^* = \frac{4-d}{12/d-5}$ same as g_1^*, shown in Fig. 1. Notice that the nontrivial fixed point diverges at $d = 12/5$ and physically unacceptable between the dimensions 12/5 and 4.

We find in detail below for different dimensions:

(i) $d \leqslant 12/5$: In this regime the Gaussian FP $g_1^* = 0 = g_2^*$ is unstable. Thus g_1^* and g_2^* should be nonzero in the statistical steady state, implying relevance (in a RG sense) of the quenched disorder. The nontrivial FP is linearly stable. The scaling exponents at the stable fixed point are given below.

(A) $d = 1$: The exponents are $\chi_1 = 9/7$, $\chi_2 = 5/7$, $z = 11/7$. Thus $\chi_2 + z = 16/7 > 2$, in contrast to the pure 1D KPZ equation. The results are consistent with [9].

(B) $d = 2$: The exponents are $\chi_1 = 2$, $\chi_2 = 2$, $z = 2$. Also here $\chi_2 + z > 2$, unlike the pure KPZ equation.

(ii) Dimension $12/5 \leqslant d < 4$: For this intermediate range of dimensions, physically acceptable fixed point is only $g_1^* = 0$, $g_2^* = 0$, which, however, is an unstable fixed point. The perturbation theory apparently breaks down for $12/5 \leqslant d < 4$, which we believe is an artifact of the one-loop expansion employed here. This is similar to what we find for $3/2 < d < 2$ in the one-loop RG calculations for the pure KPZ equation; see Eq. (13) [17]. A schematic RG flow diagram is shown in Fig. 2 below.

(iii) Dimension $d = 4$: It is the lower critical dimension of the presented model here. The nonlinear couplings are marginally relevant, are shown in (25) and (26). This implies that at $d = 4$, the coupling constants flow to infinity in a finite RG time or for a finite system size, that is controlled by the precise values of the unrenormalized model parameters (and hence nonuniversal). This is reminiscent of the flow of the coupling constant at two dimensions in the pure KPZ equation.

(iv) Dimension $d > 4$: Let $d = 4 + \epsilon$, where $\epsilon > 0$ is assumed to be small. The Gaussian fixed points are now stable, corresponding to $z = 2$, $\chi_1 = 2 - d/2$, and $\chi_2 = 1 - d/2$, corresponding to asymptotically smooth phases. In addition, similar to the pure KPZ equation, we expect unstable fixed points with both g_1^*, $g_2^* \sim O(\epsilon)$, that would indicate a disorder induced roughening transition in the model. In fact, we do find $g_1^* = \epsilon/2$. This however leaves g_2 marginal. However, given the fact that $g_2^* = 0$ is a stable fixed point (along with $g_1^* = 0$), and g_1^* has an unstable fixed point that is $O(\epsilon)$, we speculate that g_2 too shows a roughening transition such that for large enough bare or unrenormalized value of g_2, it flows to infinity under renormalization. Our one-loop RG appears to be inadequate to capture this behavior; higher-order perturbation theory or numerical solutions of the dynamical equation could be useful in this regard. This further indicates that $d = 4$ is the lower critical dimension for both g_1 and g_2.

Some studies [26–30] suggest $d = 4$ as the upper critical dimension on or above which the scaling exponents from the linear theory holds, for the pure KPZ equation. But here $d = 4$ is found to be the lower critical dimension, which is higher than the lower critical dimension of the pure KPZ equation. Since the upper critical dimension of a model is higher than the lower critical dimension in most cases, we expect the upper critical dimension for Case II is to be greater than $d = 4$.

In the pure KPZ equation, the stable fixed point that governs the rough phase is inaccessible in a perturbation theory, although such a fixed point should exist on physical ground. Similarly, here too a globally stable fixed point that

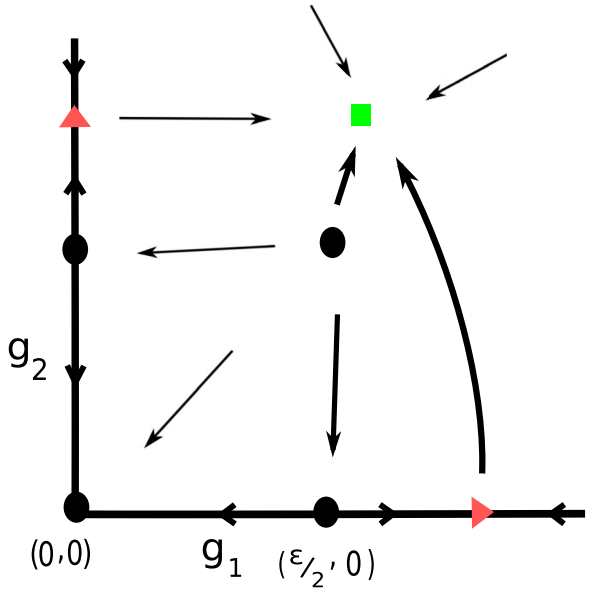

FIG. 3. Speculated global RG flows in the $g_1 - g_2$ plane in an Occam's razor style argument. Perturbative accessible (small filled black circles) and inaccessible (small coloured squares) are shown. RG flow lines with directions are marked. Notice not all the unstable and in-principle perturbatively accessible fixed points are captured by the one-loop theory; see text.

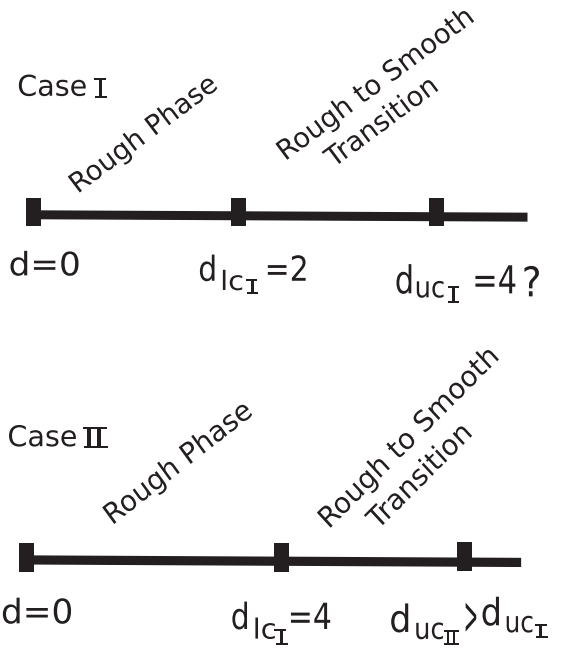

FIG. 4. Phases and phase transitions in the model as a function of d. (top) Case I and (bottom) Case II. Lower ($d_{lc_I} = 2$) and ($d_{lc_{II}} = 4$) dimensions for Case I and Case II, respectively, and (yet unknown) upper critical (d_{uc_I}) and $d_{uc_{II}}$ dimensions, respectively, for Case I and Case II are marked. Further, $d_{uc_{II}}$ is expected to be higher than d_{uc_I}; see text.

characterizes the rough phase must exist. Using an "Occam's razor" style argument, we speculate the RG flow diagram Fig. 3 that has the physically acceptable and simplest flow topology. Notice that at this putative strong coupling fixed point, both g_1 and g_2 are expected to be nonzero, for if $g_2 = 0$ at this fixed point, the rough phase should become identical to that of the pure KPZ equation. Such a possibility is, however, ruled out, since a strong coupling perturbatively inaccessible rough phase appears already at $2d$ for the pure KPZ equation, whereas for Case II here, it can appear only at $4d$ or above. Thus the rough phase here is expected to be different from its counterpart for the pure KPZ equation.

Finally, we give a schematic, pictorial comparison between the phases and phase transitions in Case I and Case II as a function of dimension d in Fig. 4 below.

We expect the new universality class that emerges in the absence of the propagating waves holds not only when these waves strictly vanish, but also when these have small amplitudes, i.e., a nonuniversal small window of speeds of propagation around zero, for reasons identical to those enunciated in Ref. [9]. Essentially for sufficiently high wave vectors, the propagating waves are subdominant to the damping terms. If under mode elimination from the high wave-vector limits, the theory gets renormalized before the crossover scale ξ_c between the propagating modes and damping terms, the renormalized theory at the crossover scale would be like what we have obtained for Case II. Since at length scales larger than ξ_c, the propagating modes are important, and no further renormalization takes place. As a result, the scaling behavior corresponding to our Case II above will be displayed by the system, with a non-KPZ scaling behavior. If, on the other hand, the theory does not get renormalized till the crossover scale ξ_c is reached, further renormalization of the theory at scales larger than ξ_c takes place, which comes entirely from the KPZ nonlinearity. This naturally leads to a scaling behavior identical to the pure KPZ equation; see Ref. [9] for more detailed discussions.

V. SUMMARY AND OUTLOOK

To summarize, we have studied here the universal scaling properties of d-dimensional KPZ equation with quenched columnar disorder. For this, we have generalized the 1D continuum equation constructed and studied in Ref. [9]. We have obtained a number of interesting results. For instance, we show that the columnar disorder in general leads to the loss of the Galilean invariance of the pure KPZ equation and generation of underdamped propagating waves in the system, which in turn makes the system anisotropic. Interestingly, these waves render the quenched disorder irrelevant (in a RG sense); as a result, the universal scaling exponents belong to the d-dimensional KPZ universality class. Since the pure KPZ equation is isotropic, this implies that the long wavelength scaling properties of the model are actually isotropic. We argue that the rough phase of the model that is inaccessible in a perturbation theory, is statistically identical to that for the pure KPZ equation in the long wavelength limit. Thus isotropy becomes an *effective* symmetry in the long wavelength limit. For certain choices of the model parameters, the propagating waves vanish. In that limit the model is already isotropic. Furthermore, the quenched disorder in the absence

of the waves is now *relevant* (in a RG sense). We establish that the model now has $d = 4$ as the *lower critical dimension*. We have calculated the roughness and the dynamic scaling exponents within a one-loop approximation, which belong to a universality class hitherto unknown. We argue that above $d = 4$ the model undergoes a roughening transition from a smooth to rough phase that is analogous to the well-known roughening transition in the KPZ equation above $d = 2$. This rough phase, although not accessible in a perturbation theory, should be statistically *different* from its counterpart in the pure KPZ equation. We have argued that the upper critical dimension in Case II should be higher than 4.

We have considered only Gaussian-distributed short-ranged quenched disorder. Our calculational framework can be extended to Gaussian-distributed long-range disorder in a straightforward manner. While precise values of the scaling exponents should depend upon the scaling of the variance of the long-range disorder, by using the logic outlined above we can generally argue that the universal scaling properties will crucially depend upon whether or not there are underdamped propagating waves. We expect our results here will provide impetus to future theoretical work along this direction.

ACKNOWLEDGMENTS

I would like to thank A. Basu (SINP, Kolkata) for helpful discussions, valuable suggestions, critical comments and continuous support to prepare the manuscript.

APPENDIX A: PERTURBATION THEORY: GENERATING FUNCTIONAL AND SCALING

The generating functional [31–35] is defined as

$$\mathcal{Z} = \int \mathcal{D}\hat{h}_1 \mathcal{D}h_1 \mathcal{D}\hat{h}_2 \mathcal{D}h_2 \mathcal{D}\delta m \exp\{-\mathcal{S}[\hat{h}_1, h_1, \hat{h}_2, h_2, \delta m]\}. \tag{A1}$$

$\hat{h}_1$, $\hat{h}_2$ are the conjugate fields to h_1, h_2 respectively. Here, $\mathcal{S}[\hat{h}_1, h_1, \hat{h}_2, h_2, \delta m]$ is the action functional. Two types of terms are present in the action $\mathcal{S}$: linear terms and nonlinear terms. The perturbation theory is set up by expanding the nonlinear terms present in the action.

The perturbative step of evaluating fluctuation corrections is followed by rescaling wave vector (equivalently, space) and frequency (equivalently, time) as $\mathbf{q} \to b\mathbf{q}$ and $\omega \to b^z\omega$, respectively. The long wavelength parts of the fields are rescaled as follows:

$$\begin{aligned}
\hat{h}_1(\mathbf{q}) &= b^{-\chi_1 - d}\hat{h}_1(b\mathbf{q}), \;\; h_1(\mathbf{q}) = b^{d+\chi_1}h_1(b\mathbf{q}),\\
\delta m(\mathbf{q}) &= b^{d/2}\delta m(b\mathbf{q}),\\
\hat{h}_2(\mathbf{q},\omega) &= b^{z-\chi_2}\hat{h}_2(b\mathbf{q}, b^z\omega),\\
h_2(\mathbf{q},\omega) &= b^{d+z+\chi_2}h_2(b\mathbf{q}, b^z\omega).
\end{aligned} \tag{A2}$$

APPENDIX B: RENORMALIZATION GROUP ANALYSIS FOR CASE I

The action functional corresponding to equations (18) and (19) is

$$\begin{aligned}
\mathcal{S}[\hat{h}_1, h_1, \hat{h}_2, h_2, \delta m] = &\int_{\mathbf{x}} \hat{h}_1[-\nu_\psi \nabla^2 h_1 - \lambda_{1\psi}\partial_\parallel h_1 - \lambda_m \delta m + \frac{\lambda_\psi}{2}(\nabla h_1)^2 - \lambda_{2\psi}[\delta m(\partial_\parallel h_1)] + \frac{\delta m^2}{4\tilde{D}}\\
&+ \int_{\mathbf{x},t} \hat{h}_2[-D\hat{h}_2 + \partial_t h_2 - \nu_\rho \nabla^2 h_2 - \lambda_{1\rho}\partial_\parallel h_2 + \frac{\lambda_\rho}{2}(\nabla h_2)^2 - \lambda_{2\rho}[\delta m(\partial_\parallel h_2)] + \lambda_{\rho\psi}(\nabla h_1)\cdot(\nabla h_2)].
\end{aligned} \tag{B1}$$

The two point functions found from linear terms present in (B1) and nonlinear vertices in (B1) are presented diagrammatically in Fig. 5 and Fig. 6, respectively.

The bare two point functions in the harmonic theory neglecting nonlinear terms from (B1) are

$$\langle \hat{h}_1(-\mathbf{k}) h_1(\mathbf{k})\rangle = \frac{1}{\nu_\psi k^2 + ik_\parallel \lambda_{1\psi}}. \tag{B2a}$$

$$\langle |h_1(\mathbf{k})|^2\rangle = \frac{2\tilde{D}\lambda_m^2}{k_\parallel^2\lambda_{1\psi}^2 + \nu_\psi^2 k^4}. \tag{B2b}$$

$$\langle h_1(-\mathbf{k})\delta m(\mathbf{k})\rangle = \frac{2\tilde{D}\lambda_m}{\nu_\psi k^2 - ik_\parallel \lambda_{1\psi}}. \tag{B2c}$$

$$\langle \hat{h}_2(-\mathbf{k},-\omega) h_2(\mathbf{k},\omega)\rangle = \frac{1}{-i\omega + ik_\parallel\lambda_{1\rho} + \nu_\rho k^2}. \tag{B2d}$$

$$\langle |h_2(\mathbf{k},\omega)|^2\rangle = \frac{2D}{(\omega - k_\parallel\lambda_{1\rho})^2 + \nu_\rho^2 k^4}. \tag{B2e}$$

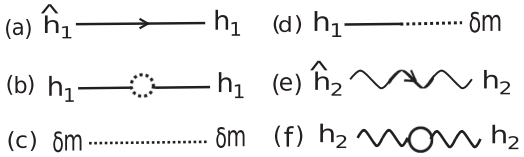

FIG. 5. Diagrammatic representations of two point functions. Arrows in propagators [(a), (e)] constitute casuality information.

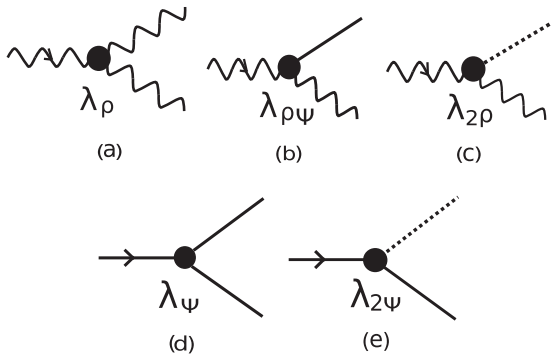

FIG. 6. Diagrammatic representations of the anharmonic vertices terms in action (B1).

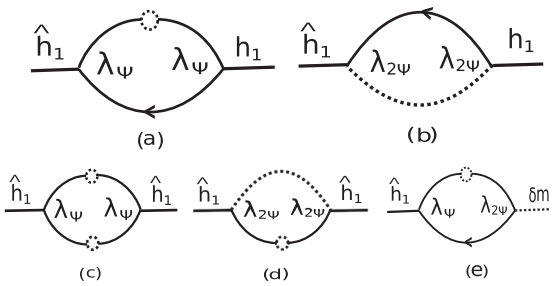

FIG. 7. One loop Feynman diagrams for the corrections of the propagator and correlator of h_1: (a), (b) for propagator and (c), (d), (e) for correlator corrections.

The fluctuation corrections of the propagators and correlators of h_1, h_2 are represented by one-loop Feynman diagrams in Fig. 7 and Fig. 8, respectively.

The one-loop contributions to the corrections of parameters in (B1) are finite. Those are of the forms

$$\text{Fig. 7(a)} = \frac{\lambda_\psi^2 \tilde{D}\lambda_m^2}{i\lambda_{1\psi}^3}\int \frac{d^d\mathbf{q}}{(2\pi)^d}\frac{1}{q_\parallel^3}[k^2q^2+(\mathbf{k}\cdot\mathbf{q})^2 - q^2\mathbf{k}\cdot\mathbf{q}(2+3k_\parallel/q_\parallel)]. \tag{B3a}$$

$$\text{Fig. 7(b)} = \frac{2\lambda_{2\psi}^2\tilde{D}}{\lambda_{1\psi}}\int\frac{d^d\mathbf{q}}{(2\pi)^d}. \tag{B3b}$$

$$\text{Fig. 7(c)} = \frac{\lambda_\psi^2(\tilde{D}\lambda_m^2)^2}{\lambda_{1\psi}^4}\int\frac{d^d\mathbf{q}}{(2\pi)^d}. \tag{B3c}$$

$$\text{Fig. 7(d)} = \frac{2\lambda_{2\psi}^2\tilde{D}^2\lambda_m^2}{\lambda_{1\psi}^2}\int\frac{d^d\mathbf{q}}{(2\pi)^d}. \tag{B3d}$$

$$\text{Fig. 7(e)} = \frac{2\lambda_\psi\lambda_{2\psi}\tilde{D}\lambda_m^2}{\lambda_{1\psi}^3}\int\frac{d^d\mathbf{q}}{(2\pi)^d}\frac{q^2}{q_\parallel^2}. \tag{B3e}$$

$$\text{Fig. 8(a)} = \frac{2D\tilde{D}\lambda_{\rho\psi}^2\lambda_m^2}{\lambda_{1\rho}^2\lambda_{1\psi}^2}\int\frac{d^d\mathbf{q}}{(2\pi)^d}\frac{q^2}{q_\parallel^2}. \tag{B4a}$$

$$\text{Fig. 8(b)} = -\frac{2D\lambda_{2\rho}^2}{\lambda_{1\rho}^2}\int\frac{d^d\mathbf{q}}{(2\pi)^d}\frac{q_\parallel^2}{q^2}. \tag{B4b}$$

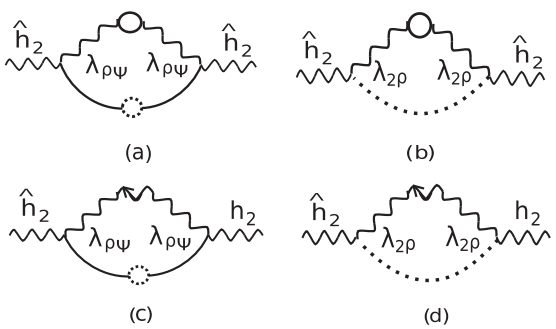

FIG. 8. One loop Feynman diagrams for the corrections of the correlator and propagator of h_2: (a), (b) for correlator and (c), (d) for propagator corrections.

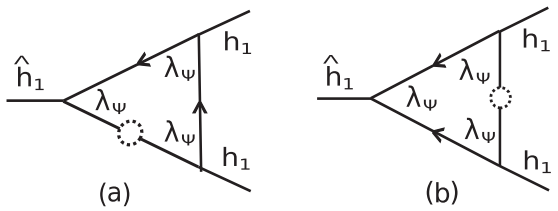

FIG. 9. One-loop Feynman diagram for the vertex λ_ψ correction for Case II.

$$\text{Fig. 8(c)} = \frac{i\tilde{D}\lambda_{\rho\psi}^2\lambda_m^2}{\lambda_{1\rho}\lambda_{1\psi}^2}\int\frac{d^d\mathbf{q}}{(2\pi)^d}\frac{1}{qq_\parallel^2}[-2(\mathbf{k}\cdot\mathbf{q})^2-k^2q^2] + \frac{q(\mathbf{k}\cdot\mathbf{q})}{q_\parallel^2}[2+k/q+k_\parallel/q_\parallel]. \tag{B4c}$$

APPENDIX C: RENORMALIZATION GROUP ANALYSIS FOR CASE II

Action functional corresponding to Eqs. (22) and (23) is

$$\mathcal{S} = \int_{\mathbf{x}}\hat{h}_1[-\nu_\psi\nabla^2h_1-\lambda_m\delta m+\frac{\lambda_\psi}{2}(\nabla h_1)^2]+\frac{\delta m^2}{4\tilde{D}} + \int_{\mathbf{x},t}\hat{h}_2[-D\hat{h_2}+(\partial_t h_2-\nu_\rho\nabla^2h_2+\lambda_{\rho\psi}\nabla h_1\cdot\nabla h_2)]. \tag{C1}$$

Two point functions of the harmonic theory neglecting nonlinear terms fom (C1) are

$$\langle\hat{h}_1(-\mathbf{k})h_1(\mathbf{k})\rangle = \frac{1}{\nu_\psi k^2}. \tag{C2a}$$

$$\langle|h_1(\mathbf{k})|^2\rangle = \frac{2\tilde{D}\lambda_m^2}{\nu_\psi^2k^4}. \tag{C2b}$$

$$\langle h_1(-\mathbf{k})\delta m(\mathbf{k})\rangle = \frac{2\tilde{D}\lambda_m}{\nu_\psi k^2}. \tag{C2c}$$

$$\langle\hat{h}_2(-\mathbf{k},-\omega)h_2(\mathbf{k},\omega)\rangle = \frac{1}{-i\omega+\nu_\rho k^2}. \tag{C2d}$$

$$\langle|h_2(\mathbf{k},\omega)|^2\rangle = \frac{2D}{\omega^2+\nu_\rho^2k^4}. \tag{C2e}$$

The two point functions for this case are also represented diagrammatically in Fig. 5. For this case, the nonlinear vertices are presented by Figs. 6(a), 6(b), and 6(d).

In this case, the one loop diagrams in Figs. 7(a), 7(c) contribute to the corrections of the propagator and correlator of h_1, respectively. The diagrams in Figs. 8(a), 8(c) contribute to the corrections of correlator and propagator of h_2, respectively. Figures 9 and 10 contribute to vertices corrections in (C1).

The one-loop contributions to corrections of parameters in (C1) are

$$\text{Fig. 7(a)} = \frac{\lambda_\psi^2\tilde{D}\lambda_m^2}{\nu_\psi^3}\left[\frac{2}{d}-1\right]\int_{\Lambda/b}^{\Lambda}\frac{d^d\mathbf{q}}{(2\pi)^d}\frac{1}{q^4}. \tag{C3a}$$

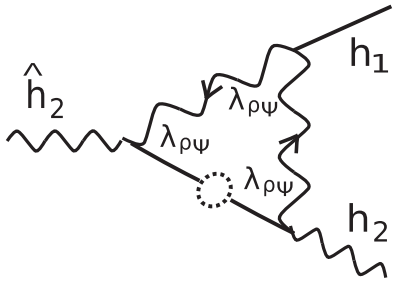

FIG. 10. One-loop Feynman diagram for the vertex $\lambda_{\rho\psi}$ correction for Case II.

$$\text{Fig. 7(c)} = \frac{\lambda_\psi^2 \tilde{D}^2 \lambda_m^2}{\nu_\psi^4} \int_{\Lambda/b}^{\Lambda} \frac{d^d\mathbf{q}}{(2\pi)^d} \frac{1}{q^4}. \tag{C3b}$$

$$\text{Fig. 8(a)} = \frac{2D\lambda_{\rho\psi}^2 \tilde{D}\lambda_m^2}{\nu_\psi^2 \nu_\rho^2} \int_{\Lambda/b}^{\Lambda} \frac{d^d\mathbf{q}}{(2\pi)^d} \frac{1}{q^4}. \tag{C4a}$$

$$\text{Fig. 8(c)} = \frac{\lambda_{\rho\psi}^2 \tilde{D}\lambda_m^2}{\nu_\psi^2 \nu_\rho} [1 - 2/d] \int_{\Lambda/b}^{\Lambda} \frac{d^d\mathbf{q}}{(2\pi)^d} \frac{1}{q^4}. \tag{C4b}$$

$$\text{Fig. 9(a)} = \frac{2\lambda_\psi^3 \tilde{D}\lambda_m^2}{\nu_\psi^4 d} \int_{\Lambda/b}^{\Lambda} \frac{d^d\mathbf{q}}{(2\pi)^d} \frac{1}{q^4}. \tag{C5a}$$

$$\text{Fig. 9(b)} = -\frac{\lambda_\psi^3 \tilde{D}\lambda_m^2}{\nu_\psi^4 d} \int_{\Lambda/b}^{\Lambda} \frac{d^d\mathbf{q}}{(2\pi)^d} \frac{1}{q^4}. \tag{C5b}$$

$$\text{Fig. 10} = \frac{2\lambda_{\rho\psi}^3 \tilde{D}\lambda_m^2}{\nu_\psi^2 \nu_\rho^2 d} \int_{\Lambda/b}^{\Lambda} \frac{d^d\mathbf{q}}{(2\pi)^d} \frac{1}{q^4}. \tag{C6}$$

Finally one-loop corrected parameters in (C1) are

$$\nu_\psi^< = \nu_\psi \left[1 + \left(\frac{2}{d} - 1 \right) \frac{\lambda_\psi^2 \tilde{D}\lambda_m^2}{\nu_\psi^4} \int_{\Lambda/b}^{\Lambda} \frac{d^d\mathbf{q}}{(2\pi)^d} \frac{1}{q^4} \right]. \tag{C7a}$$

$$\lambda_m^< = \lambda_m \left[1 + \frac{\lambda_\psi^2 \tilde{D}\lambda_m^2}{2\nu_\psi^4} \int_{\Lambda/b}^{\Lambda} \frac{d^d\mathbf{q}}{(2\pi)^d} \frac{1}{q^4} \right]. \tag{C7b}$$

$$\lambda_\psi^< = \lambda_\psi \left[1 - \frac{\lambda_\psi^2 \tilde{D}\lambda_m^2}{\nu_\psi^4} \frac{2}{d} \int_{\Lambda/b}^{\Lambda} \frac{d^d\mathbf{q}}{(2\pi)^d} \frac{1}{q^4} \right]. \tag{C7c}$$

$$\nu_\rho^< = \nu_\rho \left[1 + \left(\frac{2}{d} - 1 \right) \frac{\lambda_{\rho\psi}^2 \tilde{D}\lambda_m^2}{\nu_\psi^2 \nu_\rho^2} \int_{\Lambda/b}^{\Lambda} \frac{d^d\mathbf{q}}{(2\pi)^d} \frac{1}{q^4} \right]. \tag{C7d}$$

$$D^< = D \left[1 + \frac{2\lambda_{\rho\psi}^2 \tilde{D}\lambda_m^2}{\nu_\psi^2 \nu_\rho^2} \int_{\Lambda/b}^{\Lambda} \frac{d^d\mathbf{q}}{(2\pi)^d} \frac{1}{q^4} \right]. \tag{C7e}$$

$$\lambda_{\rho\psi}^< = \lambda_{\rho\psi} \left[1 - \frac{\lambda_{\rho\psi}^2 \tilde{D}\lambda_m^2}{\nu_\psi^2 \nu_\rho^2} \frac{2}{d} \int_{\Lambda/b}^{\Lambda} \frac{d^d\mathbf{q}}{(2\pi)^d} \frac{1}{q^4} \right]. \tag{C7f}$$

[1] T. C. Lubensky, Critical properties of random-spin models from the ε-expansion, Phys. Rev. B **11**, 3573 (1975).

[2] S. Mukherjee and A. Basu, Dynamic scaling in the quenched disordered classical n-vector model, Phys. Rev. Research **2**, 033423 (2020).

[3] G. Grinstein and A. Luther, Application of the renormalization group to phase transitions in disordered systems, Phys. Rev. B **13**, 1329 (1976).

[4] H. Jeong, B. Kahng, and D. Kim, Anisotropic Surface Growth Model in Disordered Media, Phys. Rev. Lett. **77**, 5094 (1996).

[5] Z. Csahók, K. Honda, E. Somfai, M. Vicsek, and T. Vicsek, Dynamics of surface roughening in disordered media, Physica A **200**, 136 (1993).

[6] A.-L. Barabási, G. Grinstein, and M. A. Munoz, Directed Surfaces in Disordered Media, Phys. Rev. Lett. **76**, 1481 (1996).

[7] L. N. Amaral, A.-L. Barabási, and H. E. Stanley, Universality Classes for Interface Growth with Quenched Disorder, Phys. Rev. Lett. **73**, 62 (1994).

[8] M. Kardar, G. Parisi, and Y. C. Zhang, Dynamic Scaling of Growing Interfaces, Phys. Rev. Lett. **56**, 889 (1986).

[9] A. Haldar and A. Basu, Marching on a rugged landscape: Universality in disordered asymmetric exclusion processes, Phys. Rev. Research **2**, 043073 (2020).

[10] G. Tripathy and M. Barma, Steady State and Dynamics of Driven Diffusive Systems with Quenched Disorder, Phys. Rev. Lett. **78**, 3039 (1997).

[11] G. Tripathy and M. Barma, Driven lattice gases with quenched disorder: Exact results and different macroscopic regimes, Phys. Rev. E **58**, 1911 (1998).

[12] S. L. A. de Queiroz and R. B. Stinchcombe, Nonequilibrium processes: Driven lattice gases, interface dynamics, and quenched-disorder effects on density profiles and currents, Phys. Rev. E **78**, 031106 (2008).

[13] E. Altman, L. M. Sieberer, L. Chen, S. Diehl, and J. Toner, Two-Dimensional Superfluidity of Exciton Polaritons Requires Strong Anisotropy, Phys. Rev. X **5**, 011017 (2015).

[14] A.-L. Barabási and H. E. Stanley, *Fractal Concepts in Surface Growth* (Cambridge University Press, Cambridge, 1995).

[15] D. Forster, D. R. Nelson, and M. J. Stephen, Large-distance and long-time properties of a randomly stirred fluid, Phys. Rev. A **16**, 732 (1977).

[16] J. Bec and K. Khanin, Burgers turbulence, Phys. Rep. **447**, 1 (2007).

[17] E. Frey and U. C. Täuber, Two-loop renormalization-group analysis of the Burgers–Kardar-Parisi-Zhang equation, Phys. Rev. E **50**, 1024 (1994).

[18] J. Quastel and H. Spohn, The one-dimensional KPZ equation and its universality class, J. Stat. Phys. **160**, 965 (2015).

[19] T. Halpin-Healy and K. A. Takeuchi, A KPZ cocktail-shaken, not stirred..., J. Stat. Phys. **160**, 794 (2015).

[20] K. A. Takeuchi, An appetizer to modern developments on the Kardar-Parisi-Zhang universality class, Physica A **504**, 77 (2018).

[21] I. Corwin, The Kardar-Parisi-Zhang equation and universality class, Random Matrices: Theory Appl. **1**, 1130001 (2012).

[22] L. Canet, H. Chaté, B. Delamotte, and N. Wschebor, Nonperturbative renormalization group for the Kardar-Parisi-Zhang

equation: General framework and first applications, Phys. Rev. E **84**, 061128 (2011).

[23] S. Mathey, E. Agoritsas, T. Kloss, V. Lecomte, and L. Canet, Kardar-Parisi-Zhang equation with short-range correlated noise: Emergent symmetries and nonuniversal observables, Phys. Rev. E **95**, 032117 (2017).

[24] O. Niggemann and H. Hinrichsen, Sinc noise for the Kardar-Parisi-Zhang equation, Phys. Rev. E **97**, 062125 (2018).

[25] P. M Chaikin and T. C Lubensky, *Principles of Condensed Matter Physics* (Cambridge University Press, Cambridge, 2000), Vol. 1.

[26] M. Lässig and H. Kinzelbach, Upper Critical Dimension of the Kardar-Parisi-Zhang Equation, Phys. Rev. Lett. **78**, 903 (1997).

[27] J. K. Bhattacharjee, Upper critical dimension of the Kardar-Parisi-Zhang equation, J. Phys. A: Math. Gen. **31**, L93 (1998).

[28] K. Moser, J. Kertész, and D. E Wolf, Numerical solution of the Kardar-Parisi-Zhang equation in one, two and three dimensions, Physica A **178**, 215 (1991).

[29] E. Marinari, A. Pagnani, G. Parisi, and Z. Rácz, Width distributions and the upper critical dimension of Kardar-Parisi-Zhang interfaces, Phys. Rev. E **65**, 026136 (2002).

[30] K. J. Wiese, On the perturbation expansion of the KPZ equation, J. Stat. Phys. **93**, 143 (1998).

[31] Jean Zinn-Justin, *Quantum Field Theory and Critical Phenomena*, Vol. 113 (Clarendon Press, Oxford, 2002).

[32] U. C. Täuber, *Critical Dynamics: A Field Theory Approach to Equilibrium and Non-Equilibrium Scaling Behavior* (Cambridge University Press, Cambridge, 2014).

[33] C. DeDominicis and P. C. Martin, Energy spectra of certain randomly-stirred fluids, Phys. Rev. A **19**, 419 (1979).

[34] R. Bausch, H.-K. Janssen, and H. Wagner, Renormalized field theory of critical dynamics, Z. Phys. B **24**, 113 (1976).

[35] P. C. Martin, E. D. Siggia, and H. A. Rose, Statistical dynamics of classical systems, Phys. Rev. A **8**, 423 (1973).